SLAC-PUB-7960
September 1998

Recent Developments on Strained Photocathode Research*

T. Maruyama, J. E. Clendenin, E. L. Garwin, R. E. Kirby,
G. Mulhollan, C. Y. Prescott, and H. Tang

Stanford Linear Accelerator Center
Stanford University, Stanford, CA 94309

R. Mair and R. Prepost

University of Wisconsin, Madison, WI 53706

Presented at the
Low Energy Polarized Electron Workshop
St. Petersburg, Russia
September 2-5, 1998

* Work supported by Department of Energy contract DE-AC03-76SF00515

RECENT DEVELOPMENTS ON STRAINED PHOTOCATHODE RESEARCH*

T. Maruyama[1], J. E. Clendenin[1], E. L. Garwin[1], R. E. Kirby[1], R. Mair[2], G. Mulhollan[1], R. Prepost[2], C. Y. Prescott[1], and H. Tang[1]

(1) Stanford Linear Accelerator Center, Stanford, California USA
(2) University of Wisconsin, Madison, Wisconsin USA

ABSTRACT For the past five years, strained GaAs photocathodes have been used for the SLAC polarized electron source producing electron beams having a spin polarization of 78% (85%) for high (low) current operation. Photocathode research has been continuously conducted to understand the cathode characteristics and to improve performances. This paper describes the recent developments in the strained photocathode research at SLAC.

1. INTRODUCTION

When a thin layer of GaAs is grown epitaxially on a substrate material possessing a slightly smaller lattice constant such as GaAsP, the lattice mismatch is accommodated by a coherent biaxial compressive strain within the GaAs layer. The strain alters the band structure of GaAs such that the strain dependent energy difference of the heavy-hole and light-hole bands relative to the conduction band is given by,

$$E_0^{C,HH} = E_0 + \delta E_H - \delta E_S \qquad (1)$$
$$E_0^{C,LH} = E_0 + \delta E_H + \delta E_S - (\delta E_S)^2/2\,\Delta_0, \qquad (2)$$

where E_0 is the direct band gap of fully relaxed GaAs and Δ_0 is the spin orbit splitting. The quantities E_H and E_S represent the hydrostatic shift of the center of gravity of the $P_{3/2}$ multiplet and the linear splitting of the $P_{3/2}$ multiplet respectively, and are given in terms of the biaxial strain, $\varepsilon_{\|}$, parallel to the interface by,

$$\delta E_H = 2a[(C_{11}-C_{12})/C_{11}]\varepsilon_{\|}, \text{ and}$$
$$\delta E_S = b[(C_{11}+2C_{12})/C_{11}]\varepsilon_{\|},$$

where the parameters *a* and *b* are the deformation potentials, and the C_{ij} are the elastic stiffness constants. Since the biaxial strain is compressive, the effect of the strain is to increase the band gap energy and remove the degeneracy of the heavy-hole and light-hole levels. The two important parameters in the GaAs-GaAsP structure are 1) the thickness of the GaAs layer and 2) the phosphorus fraction, x, in the $GaAs_{1-x}P_x$ buffer. While a thicker GaAs layer yields a higher quantum efficiency (QE), the strain relaxation gets larger with the thickness resulting in a lower electron-spin polarization. A larger phosphorus fraction produces a larger lattice-mismatch and therefore a larger strain. However, the GaAs thickness must be reduced to accommodate the larger lattice-mismatch.

* Work supported by Department of Energy contract DE-AC03-76SF00515

2. PHOTOCATHODE CHARACTERIZATIONS

Electron polarization and QE are measured in the cathode test system equipped with a load-lock for cathode introduction/removal and a compact medium-energy (20-30 kV) retarding-field Mott polarimeter [1]. The load-lock feature is particularly important for investigating photocathode characteristics since it eliminates the system dependence. Fig. 1 shows the cathode test system, and Fig. 2 shows a typical polarization and QE measurement as a function of the excitation wavelength. This particular sample was used for the 1997-1998 SLC run.

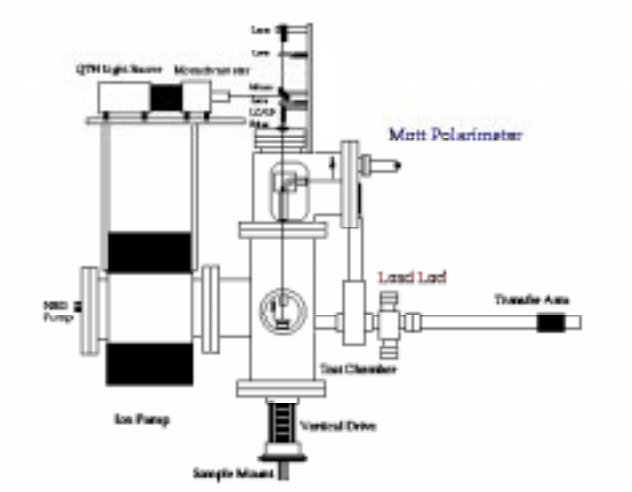

Fig. 1 The cathode test system.

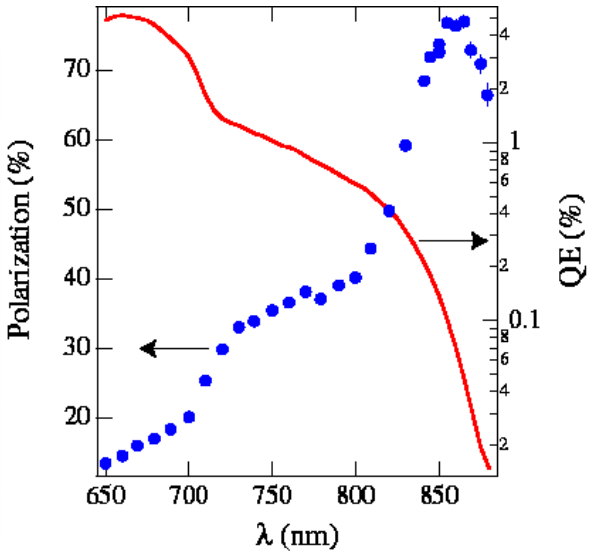

Fig. 2 Polarization and QE measurements.

X-ray diffraction is used to analyze the lattice structure. Since the strained GaAs layer has a tetragonal crystal structure, two lattice constants parallel, $a_{\parallel}$, and transverse, $a_{\perp}$, to the interface are measured. For a reflecting plane (*hkl*), the Bragg angle θ is given by,

$$\frac{2\sin\theta}{\lambda} = \sqrt{\frac{h^2+k^2}{a_{\parallel}^{\,2}} + \frac{l^2}{a_{\perp}^{\,2}}}\,.$$

Symmetric (004) and asymmetric (224) and ($2\bar{2}4$) Bragg reflections are used to measure the lattice constants $a_{\perp}$, and two lattice constants $a_{\parallel}^{[110]}$ and $a_{\parallel}^{[1\bar{1}0]}$ along [110] and [1$\bar{1}$0]. The two lattice constants along [110] and [1$\bar{1}$0] are different as a result of anisotropic strain relaxation. The transverse and parallel strains, $\varepsilon_{\perp}$ and $\varepsilon_{\parallel}$, are calculated by $\varepsilon_{\perp} = (a_{\perp} - a_0)/a_0$, and $\varepsilon_{\parallel} = (a_{\parallel} - a_0)/a_0$, where a_0 is the GaAs lattice constant.

A straightforward and useful technique for studying the band structure of a direct band gap semiconductor is through the detection of recombination radiation from optically pumped electrons [2]. Such radiation is referred to as photoluminescence (PL).

In a *p*-type GaAs crystal, electrons optically pumped across the band gap thermalize to the bottom of the conduction band before recombining with valence band holes. Therefore, the resulting PL spectrum is related to the energy dependence and separation of the participating bands. Furthermore, if the polarization states of the optical pump beam and PL are measured, additional information regarding the symmetry of valence and conduction band wave function may also be obtained. For the GaAs-GaAsP structure, two PL peaks are observed when a He-Ne laser is used for excitation. One peak observed around 850 nm is produced by the strained GaAs layer, and the peak wavelength is used to measure the band gap energy. With the presence of strain, the band gap energy shifts in a well defined manner and is directly observed as an equivalent shift of the luminescence peak. Another peak observed around 700 – 750 nm is produced by the GaAsP buffer, and the peak wavelength is used to measure the band gap energy of the GaAsP buffer. The luminescence peak position for $GaAs_{1-x}P_x$ is expected to follow $E_{PL}(x) = E_{PL}(x=0) + (1.15\ x + 0.176\ x^2)\ eV$, where $E_{PL}(x)$ is the observed luminescence peak energy, and the phosphorus fraction, x, of the $GaAs_{1-x}P_x$ layer is readily measured.

3. GaAs-GaAsP STRUCTURES [3]

In the past seven years, over 30 photocathodes of the GaAs-GaAsP structure have been investigated. The thickness of the strained GaAs layer was varied from 50 nm to 500 nm, while the phosphorus fraction in the $GaAs_{1-x}P_x$ buffer was from 20% to 33%. Most of the "production" photocathodes used for the SLAC polarized electron source were 100 nm-thick GaAs with 28-30 % phosphorus. For all these samples, polarization and QE were measured, PL spectra taken, and the lattice structure analyzed by X-ray diffraction.

Fig. 3 shows the luminescence peak position (measured in eV) of the strained GaAs layer as a function of the residual strain measured by X-ray diffraction. Since the radiative transitions are expected to be predominantly to the heavy-hole valence band, it is appropriate to compare the observed strain dependence of luminescence peak position with the expected strain dependence of the band gap of the conduction band and the heavy-hole band given by Eq. (1). The strain dependence is expected to be $\Delta E = (8.2\ \text{eV})\varepsilon_\perp$, which is consistent with the observed dependence.

Fig. 4 shows the peak electron-spin polarization as a function of the residual strain measured by X-ray diffraction. The thickness of the GaAs layer is indicated with different symbols. The peak polarization is well correlated with the measured strain. However, the highest polarization was limited to about 80 %, and the highest strain was $\varepsilon_\perp \sim 7\times10^{-3}$, which is about 80% of the designed lattice-mismatch. As the thickness of the GaAs layer was reduced, the samples showed higher polarization and strain, except for the two 50 nm-thick ones whose polarization and strain was lower than the 100 nm-thick samples. Two samples doped at $2\times10^{19}/cm^3$ show much lower polarization than all other samples doped at $5\times10^{18}/cm^3$.

A set of GaAs-GaAsP photocathodes with varying levels of strain has been used to study the following photocathode properties, 1) QE anisotropy, 2) deformation potentials for GaAs, and 3) low temperature anomalies.

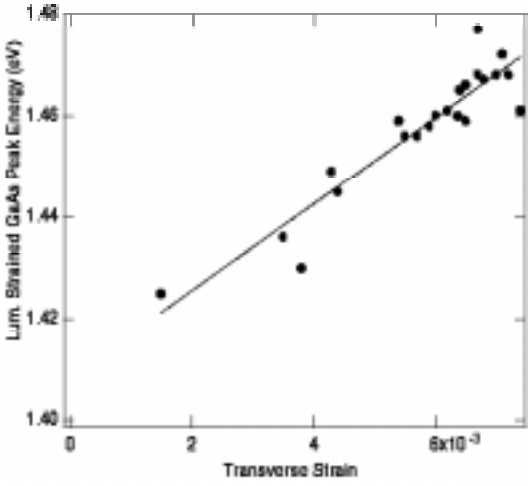

Fig. 3 PL peak energy of strained GaAs as a function of residual strain.

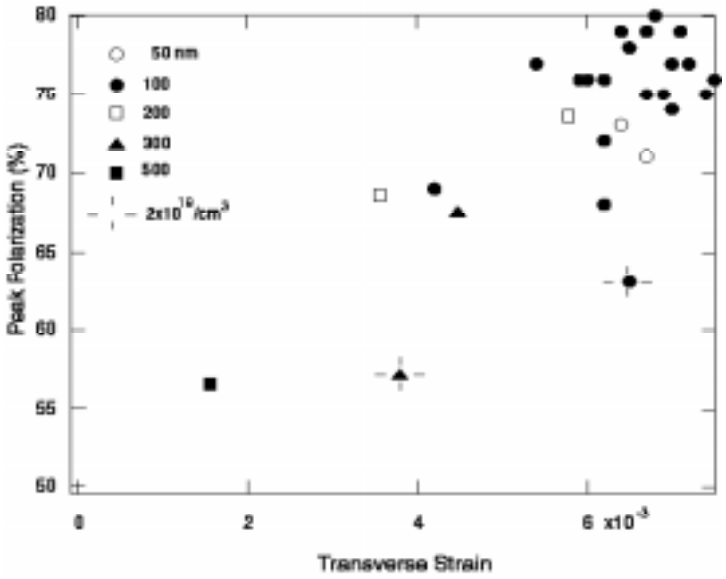

Fig. 4 Peak polarization as a function of residual strain. The different symbols indicate different GaAs thickness. All samples are doped at $5x10^{18}/cm^3$ except for the two samples doped at $2x10^{19}/cm^3$ indicated by the cross.

3.1 QE Anisotropy [4]

When a lattice-mismatched layer is grown on a substrate, the misfit is accomodated by elastic strain in the epitaxial layer. However, if the epitaxial layer exceeeds a critical thickness, the stored elastic strain in the epitaxial layer is relieved by misfit dislocations. For the zinc-blend structure, misfit dislocations develop asymmetrically along the two orthogonal directions [110] and [110], resulting in an anisotropic strain or equivalently a shear strain within the plane of the epitaxial layer. The shear strain will mix the heavy-hole and light-hole/split-off valence states and affect the optical transition probabilities. Since the mixing occurs only between opposite m_j states, if the excitation light is 100% circularly polarized, only one state can be excited and the electron-spin polarization will be unaffected. However, if the excitation light is linearly polarized, more than one state can be excited and the excitation probabilities will be dependent on the direction of linear polarization resulting in a quantum efficiency anisotropy.

Figure 5 shows the QE anisotropy as a function of the azimuthal angle of the linear polarization axis relative to the [100] direction. The maximum QE anisotropy occurs at $\phi = 135°$, implying that the maximum and minimum QE for linearly polarized light correspond to the [110] and [110] axes, respectively. Fig. 6 shows the measured

shear strain and QE anisotropy as a function of the degree of strain relaxation. For small relaxations, the generated shear appears proportional to the degree of relaxation. At some point however, the anisotropic relaxation ceases and there is movement towards an in-plane symmetric strain.

The existence of a QE anisotropy in strained layer photocathodes used for polarized electron sources may lead to helicity dependent intensity variations if there exists a small, unintentional, linear component in the circularly polarized light.

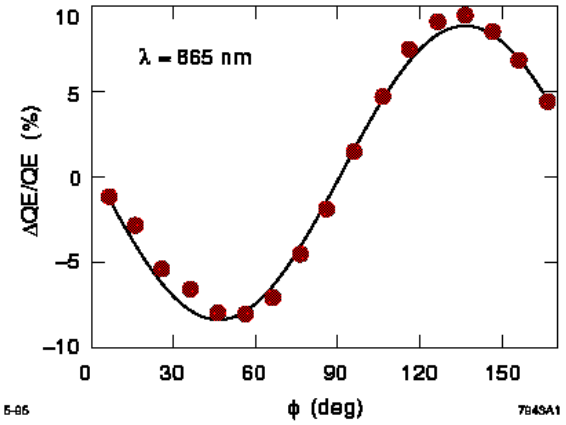

Fig. 5 QE anisotropy as a function of azimuthal angle.

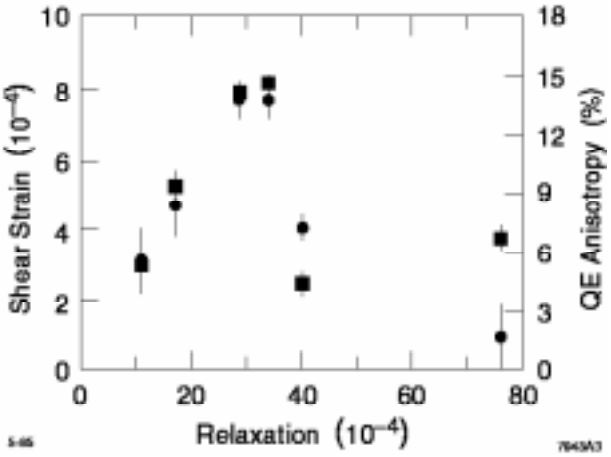

Fig. 6 Measured shear strain (circle) and QE anisotropy (square) as a function of strain relaxation.

3.2 Deformation Potential Measurement [5]

As described in Introduction, the deformation potentials relate lattice strain and the electronic band. The deformation potentials *a* and *b* for GaAs have been measured from polarized photoluminescence measurements upon a set of strained GaAs photocathodes possessing varying levels of strain. X-ray diffraction measurements yield values for the degree of lattice strain while the polarized photoluminescence measurements permit a separate determination of the heavy hole and light hole energies. Each of the samples used in this study was subjected to an etch process in order to remove the GaAs substrate. Complete removal of the GaAs substrate material was found to be critically necessary in order to obtain PL spectra from the strained GaAs layer without unwanted contributions from the substrate.

For an electron spin polarization *S* in the conduction band, the PL circular polarization associated with each of the valence bands has a magnitude *S* but is opposite in sign for each valence band. The resulting equation describing the wavelength dependence of the PL circular polarization,

$$P_{PL}(\lambda) = S\frac{(+1)I_{V_1}(\lambda)+(-1)I_{V_2}(\lambda)}{I_{V_1}(\lambda)+I_{V_2}(\lambda)},$$

is combined with the PL intensity $I_{avg} = Iv_1 + Iv_2$ to deconvolve the PL contributions from the V_1 and V_2 valence bands to yield the following equations for the individual PL contributions,

$$I_{V_1}(\lambda) = \frac{1}{2}(1 + \frac{P_{PL}(\lambda)}{S})I_{avg}(\lambda),$$

$$I_{V2}(\lambda) = \frac{1}{2}(1 - \frac{P_{PL}(\lambda)}{S})I_{avg}(\lambda).$$

The peak splitting ($Ev_1 - Ev_2$) and average peak energy ($Ec\text{-}1/2(Ev_1+Ev_2)$) are determined from the deconvolved spectra $I_{V1}(\lambda)$ and $I_{V2}(\lambda)$. The expected strain dependence of the band splitting is given by the difference of Eqs. (1) and (2) and is dependent only on the deformation potential *b*. Similarly, the expected strain dependence of the average band position is given by the average of Eqs. (1) and (2), and is dependent on the deformation potential *a* with only a very small quadratic dependence on *b*. Fig. 7 shows the PL peak splitting plotted against the transverse strain along with the best fit. From the fit, a value of $b = -2.00 \pm 0.05$ eV is found. The average PL peak energy plotted against the transverse strain is shown in Fig. 8. A best fit yielded a value of $a = -10.19 \pm 0.22$. Here, the value for b obtained from the data in Fig. 7 is used where needed.

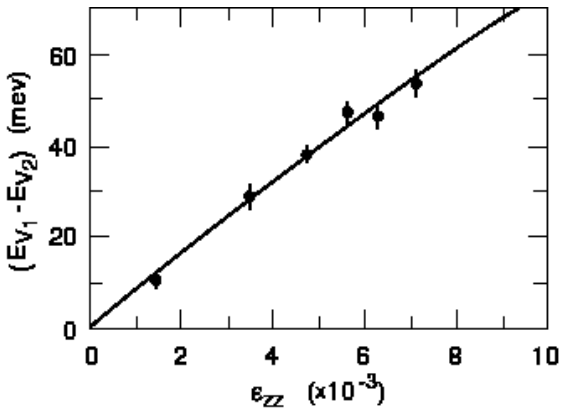

Fig. 7 Measured luminescence peak splitting against the transverse strain.

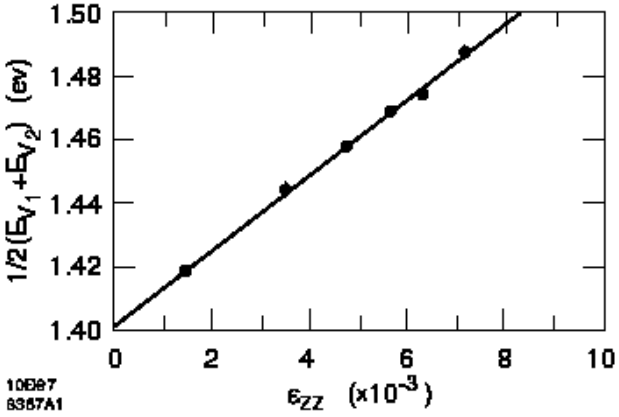

Fig. 8 Measured average luminescence peak energy against the transverse strain.

3.3 Low Temperature Anomalies

To study temperature dependence on luminescence circular polarization, luminescence measurements are performed at 78 K and 12 K. The PL spectra will shift

to shorter wavelengths upon cooling due to the temperature dependence of the band gap. Other expected temperature dependent effects are the narrowing of the PL spectra at low temperature and a more rapid enhancement in luminescence circular polarization. This is due to both a decreased level of band tailing and a smaller k_BT spread in the Fermi-distribution. This may also result in a higher circular polarization.

Fig. 9 shows the measured luminescence circular polarization as a function of pump wavelength at room temperature, 78 K, and 12K. The expected wavelength shift and sharpening of the luminescence circular polarization curve at lower temperature are both observed. Furthermore, the peak polarization increased upon cooling from room temperature to 78 K. However, the 78 K data show a region where the polarization decreases, with increasing pump wavelength, before ultimately exhibiting the characteristic strain enhancement. The small "dip" in polarization observed in the 78 K data is more pronounced in the 12 K data. In fact, the "dip" is so severe that the polarization decreases to almost zero with no overall polarization enhancement seen.

Recently German and Subashiev proposed a model which explaines the low temperature anomalies [6]. In highly *p*-doped semiconductor, the Fermi-level is located below the top of the heavy-hole band. At low temperatures where the band tailing is smaller and the top of the heavy-hole band is empty, the transitions from the light-hole band rather than from the heavy-hole band can predominate, resulting in a decreased or even an opposite-sign polarization. This effect is sensitive to temperature, doping level and band-tailing.

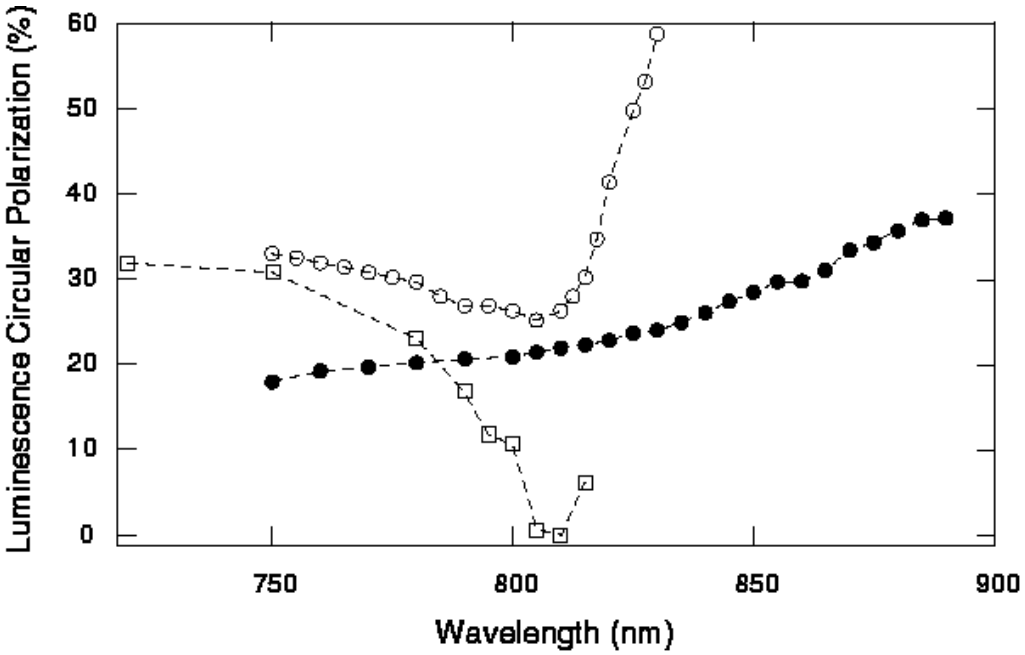

Fig. 9 Luminescence circular polarization as a function of pump wavelength at room temperature (solid circle), 78 K (open circle), and 12 K (square).

4. OTHER STRAINED HETEROSTRUCTURES

The GaAs-GaAsP photocathodes have performed extremely well producing highly polarized electrons for the e^+e^- collider experiment (SLD) as well as the fixed target experiments at SLAC. However, there is room for improvement in the electron polarization. The less-than-ideal polarizations are a result of both imperfections and depolarizations within the photocathode. Imperfections, usually in the form of strain relieving dislocations, contribute to incomplete separation of the heavy and light hole bands. From the surface morphology study and transmission electron microscopy analysis of the GaAs-GaAsP structure, it was found that the misfit dislocations and other crystal imperfections were predominantly produced in the GaAsP buffer layer. Several attempts have been made to improve the quality of the GaAsP layer. 1) After GaAsP layer growth, the growth was paused and the layer was annealed at 900° C in an attempt to reduce the number of dislocations. 2) Strain relieving superlattice $GaAs_{1-x}P_x$-$GaAs_{1-y}P_y$ was grown prior to the GaAsP buffer growth. 3) Strained GaAs was grown directly on VPE-grown Te-doped n-type GaAsP pseudo-substrates.

Other strained heterostructures have been investigated as well. 1) Instead of GaAsP, InGaP was used for the buffer layer. This structure was studied for two different substrates, GaAs and GaP. 2) Strained $GaAs_{1-x}P_x$ was grown on $GaAs_{1-y}P_y$ to test band gap shifting.

To date, none of these structures have shown better performances than the GaAs-GaAsP structure. Further studies with different cathode parameters are required.

5. CONCLUSIONS

Strained photocathode research has been continuously conducted at SLAC to understand the cathode characteristics and to improve performances. The GaAs-GaAsP structure has yielded electron polarization as high as 85%, but such high polarization is possible only when the cathode QE is less than 0.02%. When high QE is required, the maximum polarization seems to be limited to about 80%. Although several attempts have been made to overcome this limit, no structure has shown better performances than GaAs-GaAsP.

ACKNOWLEDGEMENTS

We thank H. Kawamata for assistance in the X-ray diffraction analysis of the GaAs-GaAsP samples.

REFERENCES

[1] G. A. Mulhollan, “Proceedings of the Workshop of Photocathodes for Polarized Electron Sources for Accelerators,” p. 211, SLAC-432, January 1994.
[2] R. A. Mair, Ph.D Thesis, University of Wisconsin 1996.
[3] T. Maruyama, E. L. Garwin, R. Prepost, and G. H. Zapalac, Phys. Rev. B46, 4261 (1992)
[4] R. A. Mair et al, Phys. Lett. A212, 231 (1996).
[5] R. A. Mair et al, Phys. Lett. A239, 277 (1998).
[6] E. P. German and A. V. Subashiev, JETP-Lett. 65, 867 (1997)